Multiscale extratropical barotropic variability on the subseasonal-to-seasonal timescale

Article

Published Version

It is advisable to refer to the publisher's version if you intend to cite from the work. See Guidance on citing.

To link to this article DOI: http://dx.doi.org/10.1002/qj.3676

CentAUR

Central Archive at the University of Reading

Reading's research outputs online

RESEARCH ARTICLE

Multiscale extratropical barotropic variability on the subseasonal-to-seasonal time-scale

Lina Boljka | Theodore G. Shepherd

Department of Meteorology, University of Reading, Reading, UK

Correspondence
L Boljka, Department of Atmospheric Science, Colorado State University, 1371 Campus Delivery, Fort Collins, CO 80523, USA.
Email: lina.boljka@colostate.edu

Abstract

Barotropic variability plays an important role in a variety of extratropical atmospheric processes, such as annular modes, teleconnections, and baroclinic life cycles, which occur on a wide range of time-scales. Extratropical dynamics is dominated by high-frequency (periods shorter than 10 days) transient waves, which drive barotropic variability through baroclinic life cycle events. However, other types of waves (e.g. low-frequency, with periods longer than 10 days, and stationary waves) also play an important role in shaping extratropical dynamics on various time-scales. This study uses reanalysis data in the context of the zonal momentum budget to address the relative importance of stationary, low-frequency and high-frequency waves in driving barotropic variability at high (synoptic) and low (subseasonal-to-seasonal) frequencies both locally in storm-track regions and in the zonal mean in both hemispheres. The analysis reveals that the eddy forcing of barotropic variability on synoptic time-scales is dominated by the interaction between low-frequency (and stationary) and high-frequency waves, and not by high-frequency self-interactions. On longer (subseasonal-to-seasonal) time-scales the picture is more complex, with increased importance of low-frequency self-interactions but still largely negligible high-frequency self-interactions. A better understanding of the mechanisms driving barotropic variability on subseasonal-to-seasonal time-scales may help advancing predictability on these time-scales.

KEYWORDS
annular modes, climate variability, low- and high-frequency waves, nonlinear dynamics, storm tracks

1 | INTRODUCTION

Barotropic variability in the atmosphere is a long-studied topic as it plays an important role in many atmospheric processes, such as annular modes (Thompson and Wallace, 2000; Lorenz and Hartmann, 2001; 2003), baroclinic life cycles (Simmons and Hoskins, 1978), and Rossby-wave teleconnections (Hoskins and Karoly, 1981; Wallace and Gutzler, 1981; Barnston and Livezey, 1987; Sardeshmukh and Hoskins, 1988; Wallace *et al.*, 1988; Hoskins and Ambrizzi, 1993). These processes occur on various spatial scales (e.g. planetary for teleconnections and synoptic

for baroclinic life cycles) as well as temporal scales (e.g. subseasonal to interannual time-scale for teleconnections and weekly/synoptic time-scale for baroclinic life cycles).

Barotropic variability is especially relevant for processes that have little vertical phase shift (i.e. a quasi-barotropic structure) and is mainly linked to changes in the zonal wind and eddy momentum fluxes (Lorenz and Hartmann, 2001; 2003). Similarly, there is a simple relationship between barotropic vorticity and vorticity fluxes, which are closely related to the zonal momentum budget (e.g. Vallis *et al.*, 2004). Because of the apparently simple relationship between the zonal wind and eddy momentum fluxes (and between barotropic vorticity and vorticity fluxes), many have attempted to model barotropic variability by treating the eddy forcing as white noise forcing (e.g. Newman *et al.*, 1997; Sardeshmukh *et al.*, 1997; Whitaker and Sardeshmukh, 1998) or nonlinear stirring (e.g. Lorenz and Hartmann, 2001; Vallis *et al.*, 2004), which leads to a barotropic response with a red spectrum. The eddy forcing is intended to represent the stochastic effects of baroclinic instability, which generates Rossby waves that propagate meridionally away from the source (stirring) region. This leads to meridional momentum fluxes in the opposite sense to the wave propagation (e.g. Held and Hoskins, 1985), resulting in converging momentum fluxes and acceleration of the zonal mean flow in the source region (as in baroclinic life cycles).

The approximations used in stochastic forcing studies are often linear (e.g. Whitaker and Sardeshmukh, 1998), i.e. incorporating linear stationary–transient interactions and treating high-frequency waves as white noise forcing, while neglecting other nonlinear wave–wave interactions (such as low-frequency self-interactions). While this approximation provides a very simple model and may be used for predicting the system on various time-scales, the nonlinear processes play an important role in weakening the variability on longer time-scales (Vallis *et al.*, 2004), which may limit the predictability.

From frequency considerations alone, we can expect the synoptic time-scale barotropic variability to be mainly driven by a combination of high-frequency self-interactions and interactions between low- (and stationary) and high-frequency waves, and the variability on longer time-scales to be mainly driven by a combination of low-frequency and high-frequency self-interactions (the latter associated with small differences between two high frequencies, which project onto low frequencies). This suggests that imposing high-frequency waves as white noise forcing in a linear model is only justified if these waves alone dominate the forcing of barotropic variability on all time-scales. Even though eddy covariances in the midlatitude troposphere are dominated by (white noise) baroclinic processes (which lead to barotropic

variability through the decay of the baroclinic life cycles (e.g. Simmons and Hoskins, 1978; Lau, 1988)), the barotropic forcing that results can be modified by low-frequency (and stationary) waves (Branstator, 1995; Limpasuvan and Hartmann, 2000; DeWeaver and Nigam, 2000a; 2000b), including external Rossby waves (Held *et al.*, 1985; Lorenz and Hartmann, 2003), and through an upscale energy cascade from smaller-scale (high frequency) to larger-scale (low frequency) waves (Vallis *et al.*, 2004; Novak *et al.*, 2015).

While many studies have shown the potential of the linear models for understanding synoptic (e.g. Whitaker and Sardeshmukh, 1998) and time-mean (e.g. Hoskins and Karoly, 1981; Valdes and Hoskins, 1989) flows, it is less clear to what extent they can reproduce the subseasonal-to-seasonal (hereafter S2S) variability (e.g. Newman *et al.*, 1997; Sardeshmukh *et al.*, 1997; Vallis *et al.*, 2004). Therefore, a better understanding of the S2S time-scale is necessary if we wish to extend predictability into the S2S time-scales (including the extension back from the seasonal to shorter S2S time-scales where seasonal averaging can no longer be used to extract the slowly varying predictable component). The S2S time-scales have gained a lot of interest in recent years as they have economic and social impacts as well as an important role for seamless prediction (e.g. Brunet *et al.*, 2010). We focus here on the midlatitude S2S time-scales, for which barotropic processes play a vital role (e.g. through teleconnections), and for which the relative importance of different types of waves (which has not been quantified before) may be crucial for understanding the variability and predictability on those time-scales.

The article is structured as follows. Section 2 describes the methodology, section 3 provides the theoretical background for the barotropic variability and the different types of waves that contribute to it (locally and in the zonal mean), and the results are presented in sections 4 and 5 for the zonal mean and local midlatitude barotropic variability, respectively. Conclusions are given in section 6.

2 | METHODS

2.1 | Data

The data used in this study are from the ERA-Interim observational reanalysis, which is provided by the European Centre for Medium-Range Weather Forecasts (Dee *et al.*, 2011). The data are analysed as daily mean (from four-times-daily resolution – the eddy fluxes are first computed at 6-hourly resolution and then averaged over 24 h) for the time period between 1 January 1981 and 31 December 2010 on a 0.7° horizontal grid and 27 pressure levels
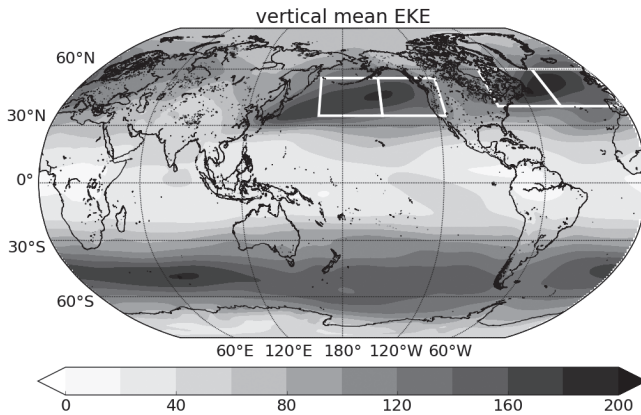
FIGURE 1   Vertically averaged annual mean EKE (in m$^2 \cdot$s^{-2}), which shows two localised storm tracks in the NH and a more zonally homogeneous Southern Hemisphere storm track. The white boxes show the upstream and downstream regions of the Pacific and Atlantic storm tracks as analysed in this article

between 1,000 and 100 hPa. All results presented below are robust to subsampling and do not change if only the cold season (winter) is considered.

The data are analysed both in a zonal mean framework (annular modes; see section 2.2) and locally in the Northern Hemisphere (NH) storm-track regions. The localised regions were defined using vertically averaged eddy kinetic energy (EKE = $0.5\langle u^{*2} + v^{*2} \rangle$), with angle brackets denoting a vertical average in pressure coordinates between 1,000 and 100 hPa, and an asterisk denoting the perturbation from the zonal mean), and were split into upstream (where EKE increases eastward) and downstream (where EKE decreases eastward) regions of the Pacific and Atlantic storm tracks (see Figure 1 and Table 1).

Note that the localised regions lie in the proximity of teleconnection patterns (e.g. Wallace and Gutzler, 1981; Barnston and Livezey, 1987), such as the West and East Pacific Oscillations (WPO and EPO, respectively), Pacific–North American (PNA) pattern and North Atlantic Oscillation (NAO). The links to these patterns are discussed in section 5 and the daily teleconnection data are provided by National Oceanic and Atmospheric Administration/Ocean and Atmosphere Research/Earth System Research Laboratory – Physical Sciences Division (NOAA/OAR/ESRL PSD) (from http://www.esrl.noaa.gov/psd/).

2.2 | Empirical orthogonal function analysis

The zonal mean component of barotropic variability is analysed using the Southern (SAM) and Northern (NAM) annular modes of variability (e.g. Thompson and Wallace, 2000). These modes are computed using empirical

orthogonal function (EOF) analysis on daily and vertically averaged zonal-mean zonal wind between 20 and 70° latitude in each hemisphere. Before computing the EOFs (and their principal components, PCs), the seasonal cycle (i.e. daily climatology, which was not smoothed) was removed from the zonal wind and the data were weighted by $\sqrt{\cos \phi}$, where ϕ is latitude. The structures of the first two EOFs in both hemispheres (hereafter SAM1 and SAM2 in the Southern Hemisphere [SH], and NAM1 and NAM2 in the NH) are shown in Figure 2, along with the normalised climatological vertically averaged zonal-mean zonal wind. SAM1 and NAM1 represent meridional shifts of the jet stream (zonal-mean zonal wind), whereas SAM2 and NAM2 represent a strengthening and narrowing of the jet stream.

Note that here (unlike in Lorenz and Hartmann (2003)) we have not removed the influence of the El Niño–Southern Oscillation, since we are computing the EOFs between 20 and 70° and not between 10 and 80° latitude, where these influences would have been more pronounced. Note also that the results do not change if the latitudinal extent is narrower (rather, the S2S time-scale results, discussed below, become even stronger).

2.3 | Spectral analysis and time filtering

2.3.1 | Cross-spectra

To examine the influence of different eddy forcings on barotropic variability on various time-scales, cross-spectrum analysis was used (Lorenz and Hartmann, 2001; 2003). We first obtained the relevant deseasonalised daily mean time series (see section 3 and text below) either by averaging over the upstream or downstream region of the storm track or by regressing the vertically and zonally averaged fields onto the EOFs of zonal-mean zonal wind (SAM1, 2, NAM1, 2). Then we divided the time series into 256-day long sections, overlapped by 128 days and windowed each section by a Hanning window, which gave at least 72 degrees of freedom. The cross-spectra were then obtained by averaging over these sections.

2.3.2 | Transient fluxes

Since the forcing of the barotropic variability can come from both stationary and transient waves, we have also computed the transient fluxes by removing the seasonal cycle (stationary component) by first subtracting the seasonal cycle from each component (e.g. separately from zonal and meridional wind) and then multiplying them to form fluxes. The transient waves (e.g. transient

TABLE 1 The upstream and downstream regions of localised storm tracks in ERA-Interim

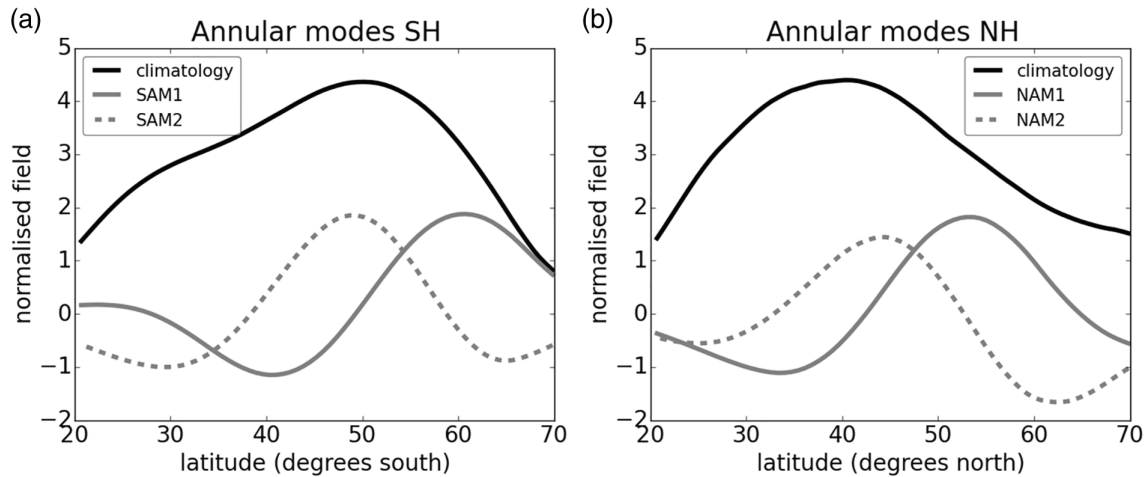|	North Atlantic	North Pacific
Upstream	40°N–60°N, 80°W–40°W	35°N–55°N, 165°E–155°W
Downstream	40°N–60°N, 40°W–0°E	35°N–55°N, 155°W–115°W

FIGURE 2 Normalised climatology of vertically and zonally averaged zonal wind (black solid line) as well as the EOF structures of the first two annular modes in the (a) SH and (b) NH. SAM1 and NAM1 are represented by a solid grey line, whereas SAM2 and NAM2 are represented by a dashed grey line. The data are normalised by their standard deviations

components of zonal and meridional wind) were further split into low- and high-frequency components using a Lanczos filter (Duchon, 1979) (again each transient component was filtered first and then multiplied to form fluxes).

When the covariability between the zonal wind and momentum fluxes due to low- or high-frequency waves is considered, the zonal wind time series is first shortened on both ends to match the Lanczos filter's data cut-off (since the filter requires a few data points at the beginning and the end of the time series to be cut off for windowing).

Note that here stationary (climatological) waves come from the seasonal cycle of the field and include the seasonal cycle as well as the stationary (long-term annual mean) components. Low-frequency waves instead are waves with time-scales longer than 10 days (which may include interannual time-scales, such as El Niño–Southern Oscillation), whereas high-frequency waves have time-scales shorter than 10 days (e.g. Hoskins et al., 1983; Limpasuvan and Hartmann, 2000). To determine the extent to which interannual variability contributes to the low-frequency waves, we have also computed the low-frequency contributions to the eddy forcing terms using a 10–90 day bandpass Lanczos filter to remove their effects. For conciseness the results are not shown, but comments are provided indicating the results of this comparison.

3 | BAROTROPIC BUDGET

To examine the barotropic variability we analyse the vertically averaged approximate zonal momentum budget (henceforth barotropic budget):

$$\frac{\partial \langle u \rangle}{\partial t} + \nabla \cdot \langle \mathbf{u}u \rangle - \langle fv \rangle = -\frac{\partial \langle \Phi \rangle}{\partial x} - \frac{\langle u \rangle}{\tau} \quad (1)$$

where u is zonal velocity, $\mathbf{u} = (u, v)$ is horizontal velocity vector, v is meridional velocity, f is Coriolis parameter, Φ is geopotential height, $\nabla \cdot$ is horizontal divergence, x is longitude, t is time and angle brackets ($\langle . \rangle$) represent the vertical average. The term $\langle u \rangle / \tau$ represents damping with τ a constant and is intended as a simple representation of surface drag and any mountain torque terms. Note that the vertical advection terms (and vertical momentum fluxes) are not present as the budget is in flux form, where these terms vanish under a vertical average. The velocities in the momentum flux ($\mathbf{u}u$) can be further split into a zonal mean (denoted with square brackets [.]) and perturbations from the zonal mean (denoted with asterisk *), yielding

$$\mathbf{u}u = \underbrace{[\mathbf{u}][u]}_{\text{zonal mean fluxes}} + \underbrace{[\mathbf{u}]u^* + \mathbf{u}^*[u]}_{\text{interaction fluxes}}^{\text{linear (in space)}} + \underbrace{\mathbf{u}^*u^*}_{\text{eddy fluxes}}^{\text{nonlinear (in space)}} . \quad (2)$$

The total barotropic budget (Equation 1) can be simplified in the zonal mean as the geopotential height gradient and the Coriolis term as well as the interaction terms in Equation 2 vanish or nearly vanish, and zonal mean fluxes contribute little (see Figure 3 below). It turns out that the eddy momentum fluxes are also the dominant contributions to barotropic variability in the storm-track regions, as the other terms in Equation 1 largely cancel out and contribute little (with the exception of the upstream Atlantic storm-track region on the S2S time-scale only; see Figure 4 below). This means that the barotropic budget can largely be simplified to (cf. Lorenz and Hartmann, 2001; 2003)

$$\frac{\partial \langle u \rangle}{\partial t} + \nabla \cdot \langle \mathbf{u}^* u^* \rangle = -\frac{\langle u \rangle}{\tau} \qquad (3)$$

both locally and in the zonal mean. Note that here the mountain torque (Lorenz and Hartmann, 2003) is not considered explicitly as it is treated as a part of the damping term, and to include it we would be including the same term twice (Hitchcock and Simpson, 2016). A small residual may be present (as in Figure 3 below) when analysing this budget due to exclusion of the Coriolis term, which is not zero under the average between 1,000 hPa and 100 hPa.

The simple budget (Equation 3) can then be analysed in frequency space to obtain the covariability of the eddy momentum flux convergence and the zonal-mean zonal wind on different time-scales. This can be achieved by taking a Fourier transform of Equation 3, yielding (cf. Lorenz and Hartmann, 2001; 2003)

$$\frac{Z^c M}{Z^c Z} = i\omega + \frac{1}{\tau}, \qquad (4)$$

where Z is the Fourier transform of $\langle u \rangle$, M is the Fourier transform of the eddy momentum flux convergence (and possibly the other forcing terms from Equation 1 as well – specified in the text where applicable), ω is the angular frequency, and the superscript c denotes complex conjugate. Following Equation 4, if the relationship between the eddy momentum flux convergence and zonal wind holds well, the imaginary part of the cross spectrum is proportional to ω, whereas the real part is constant ($=1/\tau$). That this relationship holds well for annular modes (i.e. in a zonal mean framework) has been demonstrated in Lorenz and Hartmann (2001; 2003); however, this framework can also be used to test the relative importance of different types of waves (discussed below) to the covariability of the momentum fluxes and zonal wind (as done in e.g. Blanco-Fuentes and Zurita-Gotor (2011) or Zurita-Gotor (2017) for the baroclinic budget). This provides insight into the multiscale sources of barotropic variability on different time-scales and can also provide insight into the local variability (not just the zonal mean). For brevity only the

imaginary part of the cross-spectrum will be discussed in this study (the real part of the cross-spectrum is generally a constant, representing a damping term, and therefore does not provide insight into the variability on various time-scales).

3.1 | Linear and nonlinear eddy momentum fluxes

The eddy momentum fluxes in Equation 2 can be further split into contributions from stationary (denoted with an overline) and transient (denoted with a prime) waves:

$$\mathbf{u}^* u^* = \underbrace{\overline{\mathbf{u}}^* \overline{u}^*}_{\text{stationary}} + \overbrace{\underbrace{\overline{\mathbf{u}}^* u^{*\prime} + \mathbf{u}^{*\prime} \overline{u}^*}_{\text{stationary-transient}}}^{\text{linear (in time)}} + \overbrace{\underbrace{\mathbf{u}^{*\prime} u^{*\prime}}_{\text{transient}}}^{\text{nonlinear (in time)}} . \qquad (5)$$

While eddy momentum fluxes are nonlinear in space, they can be either linear or nonlinear in time (as denoted in Equation 5). One can further consider a split in transient waves between low- and high-frequency waves (as defined in section 2), yielding

$$\mathbf{u}^{*\prime} u^{*\prime} = \underbrace{\mathbf{u}_l^{*\prime} u_l^{*\prime}}_{\text{low frequency fluxes}} + \overbrace{\mathbf{u}_l^{*\prime} u_h^{*\prime} + \mathbf{u}_h^{*\prime} u_l^{*\prime}}^{\text{low-high interaction fluxes}}$$
$$+ \underbrace{\mathbf{u}_h^{*\prime} u_h^{*\prime}}_{\text{high frequency fluxes}} . \qquad (6)$$

where subscript l refers to low-frequency waves and subscript h to high-frequency waves.

Below we address the relative importance of the stationary and transient (both low- and high-frequency) waves in forcing the barotropic variability on different time-scales both locally in the storm-track regions and in the zonal mean.

4 | ZONAL MEAN BAROTROPIC VARIABILITY

The zonal mean barotropic budget is first analysed using the annular mode framework. Figure 3 shows the cross-spectra for SAM1, 2 and NAM1, 2, representing the covariability between the zonal wind (associated with the annular modes) and the full eddy momentum flux convergence from Equation 3 (black dashed line), as well as the transient momentum flux convergence (black solid line), which was further split (as per Equation 6) into contributions from high (grey solid line) and low (grey
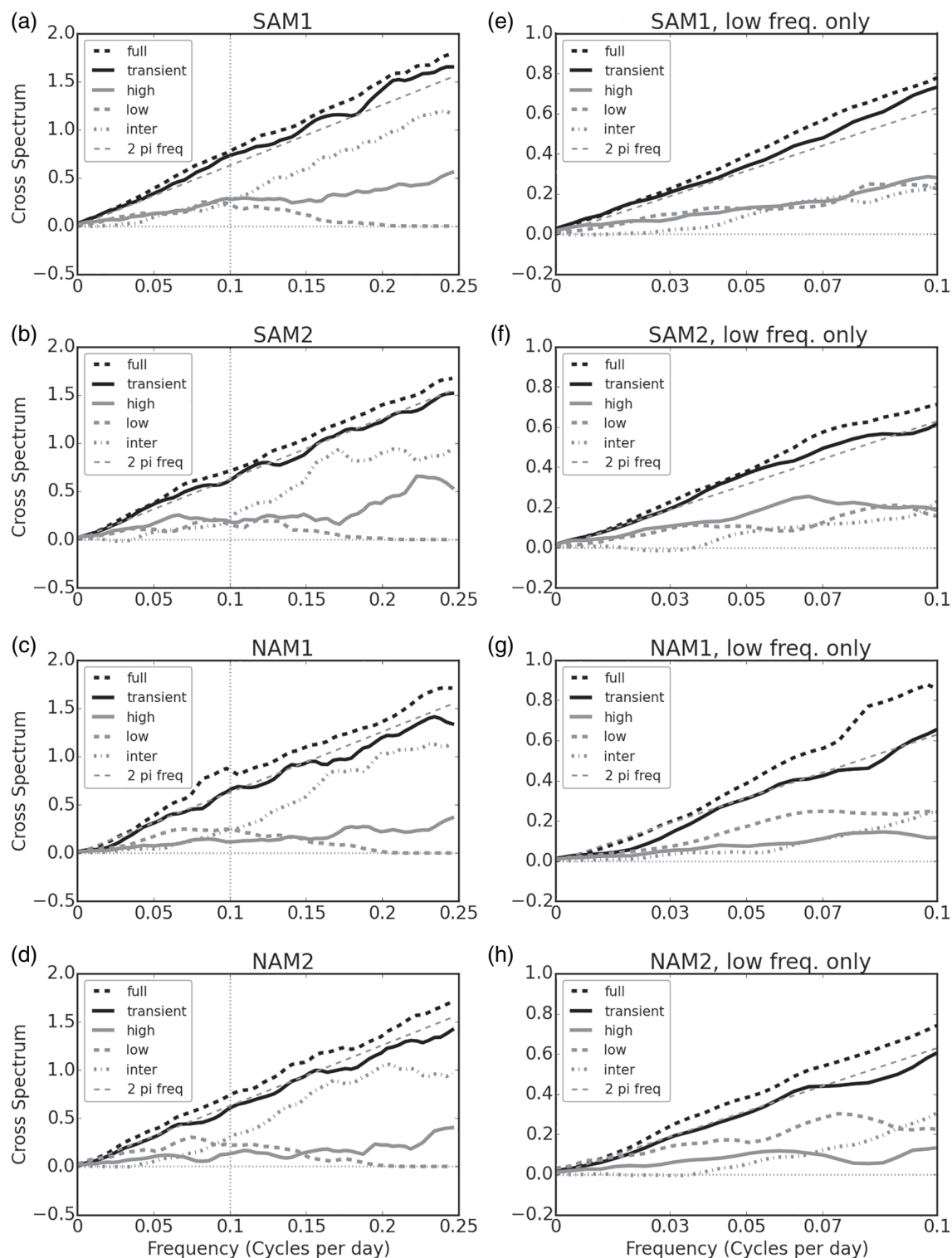
FIGURE 3 Normalised cross spectra of the idealised zonal momentum budget in (a,b,e,f) SH and (c,d,g,h) NH, with both zonal wind and eddy momentum flux convergence regressed onto EOF1 ((a,e) SAM1, (c,g) NAM1) or EOF2 ((b,f) SAM2, (d,h) NAM2) of zonal wind to obtain time series. The left column represents the full frequency range (i.e. including high frequencies), whereas the right panels show their respective variability only for periods longer than 10 days, i.e. they are a blow-up of the low-frequency (S2S) part of the spectrum which sits to the left of the thin grey vertical dotted line in the left column. Different lines in the panels represent: angular frequency (light grey dashed line), full eddy momentum flux convergence (thick black dashed line), transient eddy momentum flux convergence (thick black solid line), high-frequency eddy momentum flux convergence (thick grey solid line), low-frequency eddy momentum flux convergence (thick grey dashed line), and low–high frequency interaction eddy momentum flux convergence (thick grey dash-dotted line)
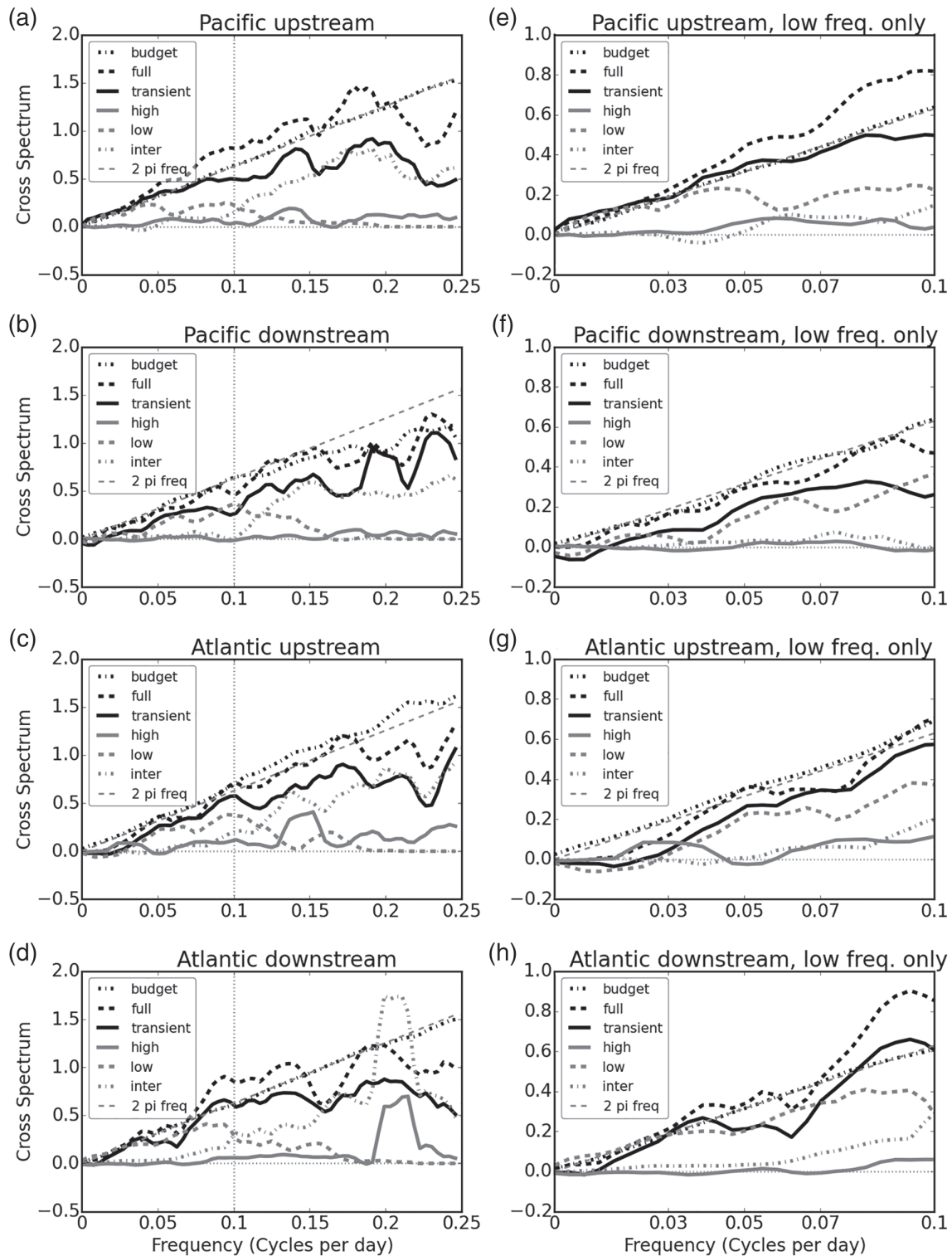
FIGURE 4 Normalised cross spectra of the idealised zonal momentum budget in the different storm-track regions: (a,e) upstream Pacific region, (b,f) downstream Pacific region, (c,g) upstream Atlantic region, and (d,h) downstream Atlantic region. Here the fields were averaged over the listed region (for definitions of the regions see Figure 1 and Table 1). Lines are the same as in Figure 3, except for the thick black dash-dotted line which represents the total zonal momentum budget forcing of Equation 1, i.e. not only the eddy momentum flux convergence, but also including the other linear terms. The left column shows the variability at all time-scales, whereas the right column shows the low-frequency variability only. Note that the large peaks present in some panels are not robust (i.e. they vanish if different lengths of segments are used before applying the spectral analysis)

dashed line) frequency waves as well as their interactions (grey dash-dotted line). The difference between the transient and full momentum flux convergence forcings of the zonal mean flow comes from the linear terms of Equation 5, i.e. via the stationary–transient interactions, but their contributions are small in a zonal mean.

The cross-spectrum analysis (Equation 4) provides a framework for analysing the covariability of two quantities on various time-scales, and if the imaginary part of the cross-spectrum follows the ω-line (thin dashed grey line), the relationship holds well (and is significant). Figure 3 clearly demonstrates that the relationship between the full eddy momentum flux convergence and zonal-mean zonal wind holds well for both annular modes in both hemispheres, and that the transient momentum fluxes dominate this relationship on all time-scales and in all cases. That the relationship of the zonal-mean zonal wind with the transient momentum flux convergence is better than the relationship with the full momentum flux convergence could mean that the stationary–transient interactions in this zonal-mean framework are balanced by the Coriolis term which is non-zero under the vertical average taken (as mentioned above).

The further split into low- and high-frequency waves and their interactions demonstrates which waves contribute to the covariability of the zonal wind and eddy momentum fluxes on different time-scales. Here we mainly consider the S2S time-scale (periods longer than 10 days and shorter than about 100 days, since the spectra are computed from 256 day-long sections, which are halved under Fourier transform) and the synoptic time-scale (periods shorter than 10 days). Note that waves of all frequencies contribute, in principle, to all time-scales of variability. Also note that none of the results below imply anything about the quasi-steady balance (not discussed in this study), which may yield different results (e.g. Boljka, 2018, figures 4.23–4.25).

On the synoptic time-scale there is a clear dominance of the eddy momentum fluxes due to low–high frequency interactions in all cases (Figure 3a–d), with no influence from the low-frequency waves alone (the latter as expected). The low-frequency component of the low–high frequency interactions is generally dominated by waves with periods shorter than 90 days, and thus not by interannual variability. Even though the high-frequency waves are mainly associated with synoptic disturbances, which are the main source of variability in the midlatitudes, the high-frequency momentum fluxes contribute little to the barotropic budget. Their importance is somewhat more pronounced in the SH where the low-frequency waves are weaker, but in the NH they do not have a prominent contribution to the budget.

The inefficiency of the high-frequency momentum fluxes in forcing the barotropic variability in the NH is also evident on S2S time-scales (Figure 3g,h), where the momentum fluxes due to low-frequency waves (including both quasi-stationary [interannual] waves and low-frequency waves with periods shorter than 90 days) dominate the driving of the barotropic variability, although the high-frequency waves are not negligible. The low-frequency wave dominance is more pronounced for NAM2 than for NAM1 and if one considers a narrower latitudinal band for the annular mode calculation, the low-frequency wave dominance on these time-scales becomes even more pronounced (for both NAM1 and NAM2; omitted for brevity). On the other hand, in the SH the high-frequency waves are equally or more important than the low-frequency waves in driving the barotropic variability on S2S time-scales (Figure 3e,f), which is especially pronounced for SAM2 (and becomes even more pronounced if a narrower latitudinal band is considered). This suggests that for SAM dynamics on S2S time-scales the low-frequency waves are less important and could potentially be excluded from the simplified models. In particular, this suggests that the results of Whitaker and Sardeshmukh (1998), where the variability is forced by high-frequency white noise forcing, could be relevant to the SH, though not to the NH. Although previous studies (e.g. Lau, 1988; Limpasuvan and Hartmann, 2000) have shown that high-frequency waves (in the SH) and stationary waves (in the NH) are important for the annular mode dynamics, they have not examined their contributions on different time-scales, which here reveals the importance of low-frequency waves on S2S time-scales and the small direct contributions from the high-frequency waves on synoptic time-scales (especially in the NH), as mentioned above. The importance of high-frequency and stationary waves becomes larger in the quasi-steady limit (Boljka, 2018).

The low-frequency wave dominance of S2S variability in the NH can be a consequence of several mechanisms: (a) the influence of external Rossby waves (Held *et al.*, 1985; Lorenz and Hartmann, 2003), (b) internal low-frequency variability of NH midlatitudes (e.g. projection of WPO, NAO, EPO, PNA on the annular mode dynamics: e.g. Ambaum *et al.*, 2001), and (c) an energy cascade from high- to low-frequency waves (e.g. Vallis *et al.*, 2004; Novak *et al.*, 2015) during the decay of a baroclinic life cycle, where barotropic processes are known to play an important role (e.g. Simmons and Hoskins, 1978). Therefore, even though the high-frequency waves may not be directly visible in Figure 3 they may have indirect effects on the barotropic variability on S2S time-scales (whereas in the SH their effect is more direct).

That the S2S variability of the NH and SH is generally driven by different types of waves shows how (dynamically) different the annular modes of the two hemispheres are on those time-scales. Also, the dominance of the transient waves in driving the barotropic variability on all time-scales suggests that annular modes are largely nonlinearly driven and hence the predictability of the barotropic variability in the zonal mean may be limited, depending on the origin of the low-frequency waves involved, some of which may provide an increased skill for predictability (e.g. via the stratosphere or Madden–Julian Oscillation events). It is worth noting that SAM1 and SAM2 appear to have similar sources of variability (similarly NAM1 and NAM2), i.e. no significant differences in their cross-spectra, which could be a consequence of SAM1 and SAM2 not being entirely independent, and represented as propagating modes of variability (Sheshadri and Plumb, 2017). Although previous work has suggested that SAM1 exhibits a positive eddy feedback (Lorenz and Hartmann, 2001) and SAM2 a stronger negative eddy feedback (Rivière *et al.*, 2016; Robert *et al.*, 2017), Byrne *et al.* (2016) has argued that these apparent eddy feedbacks inferred from lagged cross-correlations may reflect the presence of nonstationary interannual variability and be spurious.

To further investigate the NH barotropic variability (where stationary waves could be more important locally) we next perform a similar analysis in the localised storm-track regions (as defined in Figure 1 and Table 1), which provides further insight into the multiscale barotropic variability in different midlatitude regions.

5 | LOCAL BAROTROPIC VARIABILITY IN THE NH

The NH midlatitude flow (and storm-track structure) is strongly affected by local asymmetries (e.g. orography, land–sea contrasts: Brayshaw *et al.*, 2009) which force low-frequency and stationary waves, which interact with the high-frequency eddies (e.g. Hoskins *et al.*, 1983). The NH also exhibits strong local S2S variability through various (barotropic) low-frequency modes (e.g. WPO, EPO, NAO, PNA: e.g. Wallace and Gutzler, 1981; Barnston and Livezey, 1987). To better understand the relative importance of different types of waves in forcing barotropic variability locally, we now examine the two localised storm tracks in their upstream and downstream regions (Figure 1, Table 1). The zonal wind and eddy momentum flux convergence were here averaged over the region (i.e. no EOF analysis was performed as it is not as meaningful locally), before computing the cross-spectra. In addition to the analysis of the contribution of different types of waves to the momentum flux convergence (as in section

4), we also include the total budget analysis (i.e. analyse Equation 1), which adds the influence of the linear momentum fluxes (from Equation 2), Coriolis term and gradient of the geopotential height to the system – all of which are linear terms (in space). As expected, when the full budget is considered (see black dash-dotted line in Figure 4) the covariability of zonal wind and forcing follows the ω-line well. However, when only the eddy momentum fluxes are considered (i.e. analysing the simple budget (Equation 3); see black dashed line in Figure 4) the relationship between the forcing and the zonal wind is still reasonably good, suggesting that the eddy momentum fluxes dominate the zonal wind (barotropic) variability also locally, not only in the zonal mean. We use this property to assess the relative importance of stationary and transient (both low- and high-frequency) waves (as in section 4) in driving the local barotropic variability.

In contrast to the results of section 4, here the stationary–transient interaction (from Equation 5) also contributes to the barotropic budget on the synoptic time-scale (in addition to low–high frequency interactions), as seen through the difference between the lines for transient and full eddy momentum fluxes (black solid and dashed lines in Figure 4a–d), and can also be important on S2S time-scales. High-frequency waves have negligible direct contributions at all time-scales in this local perspective, even though the storm-track regions are governed by the high-frequency eddies, but may influence the barotropic variability indirectly through interactions with the low-frequency (and stationary) waves or via an upscale energy cascade (as mentioned above). The direct contribution of the high-frequency self-interactions does not increase if we average over a narrower meridional extent; rather, this reveals a larger importance of the stationary–transient interactions in the southern part of the box, and an even larger importance of low-frequency self-interactions in the northern part of the box (not shown).

The influence of stationary waves in the local budget on all time-scales suggests that locally at least a part of the variability can come from linear (in time) eddy momentum fluxes. While the synoptic variability is consistent between regions, the S2S variability is more complex and can vary from region to region.

The transient momentum fluxes on S2S time-scales are dominated by low-frequency self-interactions (including both quasi-stationary [interannual] waves and low-frequency waves with periods shorter than 90 days) in all regions (Figure 4e–h), especially when the low–high frequency interactions become less important; however, the importance of these transient momentum fluxes within the total momentum budget varies from region to region.

The S2S variability of the upstream Pacific and downstream Atlantic regions (Figure 4e,h) is dominated by transient waves and the barotropic variability in these regions is therefore largely nonlinear. The low-frequency wave dominance in these two regions may be linked respectively to the WPO and NAO indices that are the dominant low-frequency patterns in these two regions (the correlation between the zonal wind in the Pacific upstream region and WPO is 0.87, and the correlation between the zonal wind in the downstream Atlantic region and NAO is 0.80, even when using unfiltered data). The dominance of low-frequency waves (where waves with periods shorter than 90 days are found to dominate over interannual variability) on S2S time-scales also suggests that random (stochastic) forcing may not be a good approximation here (as also mentioned in e.g. Newman *et al.*, 1997), which was also the case in the zonal mean (section 4). Since the S2S variability in these two regions is dominated by low-frequency waves, one could simplify the barotropic budget (Equation 3) on these time-scales to

$$\frac{\partial \langle u \rangle}{\partial t} + \nabla \cdot \langle \mathbf{u}_l^{*\prime} u_l^{*\prime} \rangle = -\frac{\langle u \rangle}{\tau}. \tag{7}$$

Interestingly, the upstream Atlantic storm-track region shows a dominance of low-frequency transients (again dominated by waves with periods shorter than 90 days) only between the 10- and 30-day time-scale; however, on longer time-scales all eddy momentum fluxes become less important (i.e. only the covariability of the total budget and zonal wind follows the ω-line in Figure 4g), suggesting a largely linear problem with linear momentum fluxes (from Equation 2), Coriolis term and geopotential height gradient forcing the barotropic variability on those time-scales:

$$\frac{\partial \langle u \rangle}{\partial t} + \nabla \cdot \langle [\mathbf{u}][u] + [\mathbf{u}]u^* + \mathbf{u}^*[u] \rangle$$
$$- \langle fv \rangle = -\frac{\partial \langle \Phi \rangle}{\partial x} - \frac{\langle u \rangle}{\tau}. \tag{8}$$

This means that for the upstream Atlantic region, linear models (e.g. Whitaker and Sardeshmukh, 1998) may be sufficient. The zonal wind in this region is also strongly correlated with the NAO (correlation of 0.79), suggesting that a linear theory may work for the NAO (but only in this region, given that the downstream storm-track region is dominated by low-frequency transients (possibly formed via an upscale energy cascade, e.g. Novak *et al.*, 2015), even though it is also strongly correlated with the NAO as mentioned above). This is consistent with DeWeaver and Nigam (2000a; 2000b), who found that the linear terms of the momentum budget are important for the NAO.

The S2S variability in the downstream Pacific storm-track region (Figure 4f) shows a similar behaviour

to its synoptic variability, i.e. both transient and stationary waves matter, but the eddy momentum fluxes still dominate this region (i.e. linear fluxes, such as in Equation 8, are less important), meaning that Equation 3 is a good approximation to the barotropic variability here. That the stationary waves are more important in the downstream Pacific region was noted in the climate change study of Simpson *et al.* (2014), where they showed that the stationary waves are responsible for the equatorward shift of the jet stream in that region. Here we show that these waves also matter for S2S time-scales. Also, this region is linked to the EPO, which has a 0.89 correlation with the zonal wind in the downstream region of the Pacific storm track. The importance of stationary waves in this region also means that (at least in time) the barotropic variability here is partially linear. Moreover, the low-frequency waves in this region have a large component arising from the interannual variability (i.e. quasi-stationary waves), further emphasising the potential of linear approximations here.

Note that the PNA has not yet been discussed because its correlation with the zonal wind in the Pacific storm-track regions is very low (<0.3); however, the PNA has a strong correlation with the meridional wind in the downstream Pacific region (correlation of 0.82; see also Boljka, 2018). This is not surprising given that the PNA resembles a wave train pattern rather than a latitudinal shift of the midlatitude jet stream (but may be related to the subtropical jet, which is not considered here).

This section has identified the leading contributions to the local barotropic variability on S2S and synoptic time-scales. On synoptic time-scales the barotropic budget is well approximated by Equation 3; however, on S2S time-scales the picture is more complex, as the source of the forcing for the barotropic variability varies. There is a low-frequency wave dominance in the upstream Pacific and downstream Atlantic regions (see Equation 7), which is somewhat consistent with the zonal mean perspective (NAM1, 2 in section 4), whereas in the upstream Atlantic region the linear budget approximation is sufficient (see Equation 8), and in the downstream Pacific region the stationary and interannual waves play an important role (similar to the case of the synoptic variability). Even though the S2S variability is largely nonlinear, knowing which waves contribute to the variability at those time-scales may help understanding the subseasonal-to-seasonal predictability as only a simplified budget is then necessary to explain the barotropic variability on those time-scales (e.g. Equation 7).

6 | SUMMARY AND CONCLUSIONS

This study has examined the forcing of barotropic zonal-wind variability on synoptic and S2S time-scales,

from both a zonal mean and a local (storm track) perspective. A better understanding of which types of waves force the barotropic variability on different time-scales may help with predictability on those time-scales – here we mainly discussed the S2S variability.

We used the annular mode (SAM1, 2; NAM1, 2) perspective to study barotropic variability in the zonal mean. This revealed that the zonal-mean barotropic variability on all time-scales is dominated by transient waves (i.e. transient eddy momentum fluxes dominate the zonal wind forcing), which provides a largely nonlinear forcing of the flow and thus may limit its predictability. We also found that the forcing by high-frequency waves is less important in the NH than in the SH on all time-scales, and that the NH S2S variability is dominated by the forcing by low-frequency waves (though not as clearly as is the case locally). On synoptic time-scales the low–high frequency interactions dominate the budget, with only minor contributions from the high-frequency waves. However, it is important to bear in mind that the high-frequency waves can impact the barotropic variability indirectly, e.g. via an upscale energy cascade.

Locally the picture is more diverse. While on synoptic time-scales all storm-track regions considered here exhibited similar behaviour with the dominance of a combination of stationary–transient interactions and low–high frequency interactions (and negligible high-frequency self-interactions), the S2S variability showed large differences between regions.

The upstream Pacific and downstream Atlantic regions showed a clear dominance of low-frequency waves in forcing the barotropic variability, which could be related to the low-frequency modes found in these regions (WPO, NAO). This low-frequency wave forcing of the barotropic variability could be the cause of the low-frequency wave dominance in the zonal-mean framework as well (e.g. local low-frequency modes can project onto annular modes: Ambaum *et al.*, 2001). This behaviour shows the nonlinearity of barotropic variability on those time-scales; however, it also narrows the wave forcing of the barotropic variability in those regions to low-frequency waves alone (which are not necessarily random, i.e. stochastic forcing might not be appropriate in this case).

The downstream Pacific region revealed that the barotropic variability there is influenced by all classes of waves, including the stationary and quasi-stationary (interannual) waves. This means that the barotropic variability in this region could at least partially represent a linear problem (stationary–transient interactions), but this perspective cannot explain the full variability in this region. This is also the only region considered that had some influence from stationary waves on S2S time-scales.

A completely different picture, however, emerged in the upstream Atlantic region. There the barotropic variability on time-scales longer than 30 days can be represented by a linear barotropic budget (i.e. eddy momentum flux convergence has no influence on those time-scales; see Equation 8). This could be because this region is situated at the land–sea boundary where the linear terms (e.g. geopotential height gradient and linear momentum fluxes) can play a more important role than further downstream. The linearity of the barotropic budget here means that linear models (e.g. Whitaker and Sardeshmukh, 1998) could be used in this region and the variability may therefore be easier to predict. Since the wind in this region is strongly correlated with the NAO, this could also have implications for the predictability of the NAO (e.g. Molteni and Kucharski, 2019).

In summary, this study has identified the leading forcings of barotropic variability in different regions of the Earth's midlatitudes, especially on S2S time-scales, which could help further advancing its subseasonal-to-seasonal predictability. Further insight into the S2S variability (and its predictability) could be gained by exploring the origin of the low-frequency waves that contribute to the S2S variability, which is left for future work.

ORCID

Lina Boljka https://orcid.org/0000-0003-4197-9350
Theodore G. Shepherd https://orcid.org/0000-0002-6631-9968

REFERENCES

Ambaum, M.H.P., Hoskins, B.J. and Stephenson, D.B. (2001) Arctic oscillation or North Atlantic oscillation? *Journal of the Atmospheric Sciences*, 14, 3495–3507.

Barnston, A.G. and Livezey, R.E. (1987) Classification, seasonality and persistence of low-frequency atmospheric circulation patterns. *Monthly Weather Review*, 115, 1083–1126.

Blanco-Fuentes, J. and Zurita-Gotor, P. (2011) The driving of baroclinic anomalies at different timescales. *Geophysical Research Letters*, 38(23), 1–7. https://doi.org/10.1029/2011GL049785.

Boljka L. (2018) *Baroclinic and barotropic aspects of extratropical wave-mean flow interaction.* PhD Thesis, University of Reading, UK.

Branstator, G. (1995) Organization of storm track anomalies by recurring low-frequency circulation anomalies. *Journal of the Atmospheric Sciences*, 52, 207–226.

Brayshaw, D.J., Hoskins, B.J. and Blackburn, M. (2009) The basic ingredients of the North Atlantic storm track. Part I: Land–sea contrast and orography. *Journal of the Atmospheric Sciences*, 66, 2539–2558. https://doi.org/10.1175/2009JAS3078.1.

Brunet, G., Shapiro, M., Hoskins, B.J., Moncrieff, M., Dole, R., Kiladis, G.N., Kirtman, B., Lorenc, A., Mills, B., Morss, R., Polavarapu, S., Rogers, D., Schaake, J. and Shukla, J. (2010) Collaboration of the weather and climate communities to advance subseasonal-to-seasonal prediction. *Bulletin of the American Meteorological Society*, 91, 1397–1406. https://doi.org/10.1175/2010BAMS3013.1.

Byrne, N.J., Shepherd, T.G., Woollings, T. and Plumb, R.A. (2016) Annular modes and apparent eddy feedbacks in the Southern Hemisphere. *Geophysical Research Letters*, 43, 3897–3902. https://doi.org/10.1002/2016GL068851.

Dee, D.P., Uppala, S.M., Simmons, A.J., Berrisford, P., Poli, P., Kobayashi, S., Andrae, U., Balmaseda, M.A., Balsamo, G., Bauer, P., Bechtold, P., Beljaars, A.C.M., van de Berg, L., Bidlot, J., Bormann, N., Delsol, C., Dragani, R., Fuentes, M., Geer, A.J., Haimberger, L., Healy, S.B., Hersbach, H., Hólm, E.V., Isaksen, L., Kållberg, P., Köhler, M., Matricardi, M., McNally, A.P., Monge-Sanz, B.M., Morcrette, J.J., Park, B.K., Peubey, C., de Rosnay, P., Tavolato, C., Thépaut, J.N. and Vitart, F. (2011) The ERA-interim reanalysis: configuration and performance of the data assimilation system. *Quarterly Journal of the Royal Meteorological Society*, 137, 553–597. https://doi.org/10.1002/qj.828.

DeWeaver, E. and Nigam, S. (2000a) Do stationary waves drive the zonal-mean jet anomalies of the northern winter? *Journal of Climate*, 13, 2160–2176. https://doi.org/10.1175/1520-0442(2000)013<2160:DSWDTZ>2.0.CO;2.

DeWeaver, E. and Nigam, S. (2000b) Zonal-eddy dynamics of the North Atlantic Oscillation. *Journal of Climate*, 13, 3893–3914. https://doi.org/10.1175/1520-0442(2000)013<3893:ZEDOTN>2.0.CO;2.

Duchon, C.E. (1979) Lanczos filtering in one and two dimensions. *Journal of Applied Meteorology*, 19, 1016–1022.

Held, I.M. and Hoskins, B.J. (1985) Large-scale eddies and the general circulation of the troposphere. In: Saltzman, B. (Ed.) *Issues in Atmospheric and Oceanic Modeling, Advances in Geophysics*, Vol. 28A. Orlando, FL: Elsevier, pp. 3–31.

Held, I.M., Panetta, R.L. and Pierrehumbert, R.T. (1985) Stationary external Rossby waves in vertical shear. *Journal of the Atmospheric Sciences*, 42(9), 865–883.

Hitchcock, P. and Simpson, I.R. (2016) Quantifying eddy feedbacks and forcings in the tropospheric response to stratospheric sudden warmings. *Journal of the Atmospheric Sciences*, 73, 3641–3657. https://doi.org/10.1175/JAS-D-16-0056.1.

Hoskins, B.J. and Ambrizzi, T. (1993) Rossby wave propagation on a realistic longitudinally varying flow. *Journal of the Atmospheric Sciences*, 50, 1661–1671.

Hoskins, B.J., James, I.N. and White, G. (1983) The shape, propagation and mean-flow interaction of large-scale weather systems. *Journal of the Atmospheric Sciences*, 40, 1595–1612.

Hoskins, B.J. and Karoly, D.J. (1981) The steady linear response of a spherical atmosphere to thermal and orographic forcing. *Journal of the Atmospheric Sciences*, 38, 1179–1196. https://doi.org/10.1175/15200469(1981)038<1179:TSLROA>2.0.CO;2.

Lau, N.C. (1988) Variability of the observed midlatitude storm tracks in relation to low-frequency changes in the circulation pattern. *Journal of the Atmospheric Sciences*, 45, 2718–2743. https://doi.org/10.1175/1520-0469(1988)045<2718:VOTOMS>2.0.CO;2.

Limpasuvan, V. and Hartmann, D.L. (2000) Wave-maintained annular modes of climate variability. *Journal of Climate*, 13, 4414–4429. https://doi.org/10.1175/1520-0442(2000)013<4414:WMAMOC>2.0.CO;2.

Lorenz, D.J. and Hartmann, D.L. (2001) Eddy-zonal flow feedback in the Southern Hemisphere. *Journal of the Atmospheric Sciences*, 58, 3312–3327.

Lorenz, D.J. and Hartmann, D.L. (2003) Eddy-zonal flow feedback in the Northern Hemisphere winter. *Journal of Climate*, 16, 1212–1227.

Molteni, F. and Kucharski, F. (2019) A heuristic dynamical model of the North Atlantic Oscillation with a Lorenz-type chaotic attractor. *Climate Dynamics*, 52, 6173–6193. https://doi.org/10.1007/s00382-018-45094.

Newman, M., Sardeshmukh, P.D. and Penland, C. (1997) Stochastic forcing of the wintertime extratropical flow. *Journal of the Atmospheric Sciences*, 54, 435–455. https://doi.org/10.1175/15200469(1997)054<0435:SFOTWE>2.0.CO;2.

Novak, L., Ambaum, M.H.P. and Tailleux, R. (2015) The life cycle of the North Atlantic storm track. *Journal of the Atmospheric Sciences*, 72, 821–833.

Rivière, G., Robert, L. and Codron, F. (2016) A short-term negative eddy feedback on midlatitude jet variability due to planetary wave reflection. *Journal of the Atmospheric Sciences*, 73(11), 4311–4328. https://doi.org/10.1175/JAS-D-16-0079.1.

Robert, L., Rivière, G. and Codron, F. (2017) Positive and negative eddy feedbacks acting on midlatitude jet variability in a three-level quasigeostrophic model. *Journal of the Atmospheric Sciences*, 74, 1635–1649. https://doi.org/10.1175/JAS-D-16-0217.1.

Sardeshmukh, P.D. and Hoskins, B.J. (1988) The generation of global rotational flow by steady idealized tropical divergence. *Journal of the Atmospheric Sciences*, 45, 1228–1251. https://doi.org/10.1175/1520-0469(1988)045<1228:TGOGRF>2.0.CO;2.

Sardeshmukh, P.D., Newman, M. and Borges, M.D. (1997) Free barotropic Rossby wave dynamics of the wintertime low-frequency flow. *Journal of the Atmospheric Sciences*, 54, 5–23. https://doi.org/10.1175/1520-0469(1997)054<0005:FBRWDO>2.0.CO;2.

Sheshadri, A. and Plumb, R.A. (2017) Propagating annular modes: empirical orthogonal functions, principal oscillation patterns, and time scales. *Journal of the Atmospheric Sciences*, 74, 1345–1361. https://doi.org/10.1175/JAS-D-16-0291.1.

Simmons, A.J. and Hoskins, B.J. (1978) The life cycles of some nonlinear baroclinic waves. *Journal of the Atmospheric Sciences*, 35, 414–432.

Simpson, I.R., Shaw, T.A. and Seager, R. (2014) A diagnosis of the seasonally and longitudinally varying midlatitude circulation

response to global warming. *Journal of the Atmospheric Sciences*, 71, 2489–2515.

Thompson, D.W.J. and Wallace, J.M. (2000) Annular modes in the extratropical circulation. Part I: Month-to-month variability. *Journal of Climate*, 13, 1000–1016.

Valdes, P.J. and Hoskins, B.J. (1989) Linear stationary wave simulations of the time-mean climatological flow. *Journal of the Atmospheric Sciences*, 46, 2509–2527.

Vallis, G.K., Gerber, E.P., Kushner, P.J. and Cash, B.A. (2004) A mechanism and simple dynamical model of the North Atlantic Oscillation and annular modes. *Journal of the Atmospheric Sciences*, 61, 264–280.

Wallace, J.M. and Gutzler, D.S. (1981) Teleconnections in the geopotential height field during the Northern Hemisphere winter. *Monthly Weather Review*, 109, 784–812.

Wallace, J.M., Lim, G.H. and Blackmon, M.L. (1988) Relationship between cyclone tracks, anticyclone tracks and baroclinic waveguides. *Journal of the Atmospheric Sciences*, 45, 439–462.

Whitaker, J.S. and Sardeshmukh, P.D. (1998) A linear theory of extratropical synoptic eddy statistics. *Journal of the Atmospheric Sciences*, 55, 237–258. https://doi.org/10.1175/1520-0469(1998)055<0237:ALTOES>2.0.CO;2.

Zurita-Gotor, P. (2017) Low-frequency suppression of Southern Hemisphere tropospheric eddy heat flux. *Geophysical Research Letters*, 44, 2007–2015. https://doi.org/10.1002/2016GL072247.